# Comparison of relativistic bound-state calculations in Front-Form and Instant-Form Dynamics

B.L.G. Bakker, M. van Iersel, and F. Pijlman Department of Physics and AstronomyVrije Universiteit, Amsterdam, the Netherlands

November 28, 2018

#### Abstract

Using the Wick-Cutkosky model and an extended version (massive exchange) of it, we have calculated the bound states in a quantum field theoretical approach. In the light-front formalism we have calculated the bound-state mass spectrum and wave functions. Using the Terent'ev transformation we can write down an approximation for the angular dependence of the wave function. After calculating the bound-state spectra we characterized all states found. Similarly, we have calculated the bound-state spectrum and wave functions in the instant-form formalism. We compare the spectra found in both forms of dynamics in the ladder approximation and show that in both forms of dynamics the O(4) symmetry is broken.

### 1 Introduction

Dirac's paper on forms of relativistic dynamics [1] made it clear that the real difficulty of constructing a Hamiltonian theory of interacting particles that satisfies the requirements of special relativity, is finding the proper form of the interactions. This problem can be solved in a natural way by resorting to covariant field theory. Then the construction of all generators of the Poincaré group can be found in any textbook on quantum field theory. However, the results given have usually a formal meaning only and much work needs to be done to turn them into useful formulas. In particular, drastic approximations need to be taken, which may or may not be justified. An approximation that at first sight looks very attractive is to expand the states of the sytem under consideration into Fock states and truncate the expansion at a reasonable point. Doing so, one obtains a quantum-mechanical many-body problem and can use the powerfull machinery that has been developed for many-body systems.

The success of Fock-space methods depends crucially on the properties of the vacuum. Only if one can build on a simple vacuum the Fock-space expansion is useful. The condition that the vacuum be simple limits the choice of forms of dynamics in the framework of quantum field theory essentially to the front form, also known as light-front dynamics (LFD). In this form three components of the four momentum,  $p^1$ ,  $p^2$ , and  $p^+ = (p^0 + p^3)/\sqrt{2}$ , are independent of the interaction, while  $p^- = (p^0 - p^3)/\sqrt{2}$  contains interaction and is for this reason said to be a dynamical operator. The variable  $x^+ = (x^0 + x^3)/\sqrt{2}$  that is conjugate to  $p^-$ , is the evolution parameter of states and consequently denoted as light-front time. The dispersion relation of energy and momentum for a particle with mass m takes the form  $p^- = (\vec{p}_{\perp}^2 + m^2)/(2p^+), \vec{p}_{\perp} = (p^1, p^2)$ . One sees immediately that states of positive and negative energy can be separated kinematically, as positive energy and positive  $p^+$  are strictly disconnected. This property is called the *spectrum property*. In instant-form dynamics (IFD) where  $p^0$  is the dynamical component of the four momentum, the energy may be either positive or negative, independent of the three momentum. An immediate consequence of the spectrum property is that massive particles cannot be created from the vacuum in LFD. This is strictly speaking not enough to reduce the true vacuum to the perturbative Fock vacuum in LFD and usually, in order to make progress, one makes the additional assumption that zero modes, states where all particles have  $p^+=0$ , are decoupled. In this paper we shall also make this assumption. For an extensive review of many aspects of LFD we refer to Brodsky et al. [2].

Adopting LFD we still may consider other forms of dynamics, in particular IFD, for comparison. Even though it is difficult to justify IFD in a genuine field theoretical setting, to be distinguished from a situation where binding energies are very much smaller than particle masses, it remains to be seen what the quantitative differences are between the results obtained in LFD and IFD respectively. On the level of calculating invariant amplitudes in a Hamiltonian approach the situation is clear. One can obtain the time-ordered amplitudes, i.e., those that one calculates in LFD or IFD, by integrating Feynman amplitudes over the relative energy variable,  $k^-$  in LFD and  $k^0$  in IFD. Schoonderwoerd et al. [3] have shown in Yukawa theory that the difference between the covariant box diagram and the ladder approximation to it in LFD is much smaller that in IFD. As this result is obtained for the box diagram with external particles on mass shell and initial and final state on the energy shell, one cannot immediately conclude that in a bound-state calculation LFD in the ladder approximation would be closer to a covariant calculation than IFD. In this paper we show our results in the simplest possible case, the Wick-Cutkosky model (WC) [4]. (This model has been reviewed extensively by Nakanishi [5].)

The WC-model is concerned with two scalar fields,  $\Phi$  and  $\phi$ , of masses m and  $\mu$  respectively, with a coupling  $g\Phi^*\Phi\phi$ . The original WC-model has  $\mu=0$ . We study the bound-state spectrum and wave functions for a range of coupling-constant values g. Because in LFD, contrary to IFD, the components  $L_x$  and  $L_y$  of the orbital angular momentum operator  $\vec{L}$  contain interactions, manifest rotational invariance is broken in LFD. This means that if a truncation in Fock

space is made, the observables, in particular the masses of the bound states, will depend on the orientation of the light front. Below we explain how this violation of rotational invariance manifests itself in our calculations.

It is well known that the WC-model exhibits O(4) symmetry, like the non-relativistic hydrogen atom. This symmetry shows up as a degeneracy of the levels of different orbital angular momentum l. We study the breaking of this symmetry due to the ladder approximation, which amounts to the truncation to the two- and three-body sectors in Fock space. The violation of O(4) symmetry cannot be expected to occur in LFD only and we show here, for the first time, that it also occurs in IFD.

The WC-model is popular because it avoids the complications of spin and an exact solution of the Bethe-Salpeter equation is known in the case that the mass of the two-body bound state vanishes. Moreover, Cutkosky [4] gives numerical results for the spectrum in a range of values of the coupling constant. Recently, Mangin-Brinet et al. [6] calculated the ground state of the WC-model in so-called covariant LFD, also making the ladder approximation. Ji and Furn-stahl [7] estimated the masses of the 1S and 2P states in the WC-model using a variational Ansatz for the two-body wave function in LFD, for small values of the coupling constant. Ding and Darewych [8] also used variational techniques to calculate the ground state of the WC-model. In the end, they solve an equation with a kernel that does not depend on the mass of state, which may explain the fact that there masses lie much below the masses found either in the Bethe-Salpeter formalism or in the other Hamiltonian calculations.

Several authors have extended the WC-model by adopting a nonvanishing mass  $\mu$  for the exchanged particle. We mention in particular Cooke et al. [9], Nieuwenhuis and Tjon [10], and again Refs. [6, 8]. In all these works the ratio  $\mu/m = 0.15$  close to the ratio of the pion to the proton mass was taken, making these investigations relevant for the deuteron.

We consider our work as a necessary step to the treatment of more realistic models, e.g., the Yukawa model. In this domain Głazek et al. [11] have done important pioneering work in LFD. Fuda et al. [12] constructed one-boson-exchange models for the nucleon-nucleon and the pion-nucleon interactions. In the latter case an LFD calculation was compared to an IFD one. Contrary to what we do, these authors fit the parameters in the two distinct forms of dynamics separately to the experimental data, while we keep the model parameters fixed and compare the spectra.

This paper is organized as follows. In Sec.2 we give the details of the model we use and the expressions for the mass operators. Next we write down the effective two-body equations valid when Fock space is truncated to the two-and three-particle sectors. In addition we do not take self-energy terms into account, which would require a discussion of renormalization, which we want to avoid here. We do not give a detailed derivation of our equations, as e.g. Głazek et al. [11] have done so in much detail for the Yukawa model and it is easy to adapt their methods to the case of scalar particles. In Sec.3 we turn to the delicate question how to estimate the orbital angular momentum of a state in LFD, knowing that rotational invariance is broken. For the purpose

of characterizing the states we rely on Terent'ev's transformation [13], which is known to be exact for states on the energy shell [14]. For bound states, which are by definition not on shell, this transformation can only give tentative results. The next section contains the details of our numerical methods and in Sec.5 we give the masses and the wave functions we found. Finally we discuss our results and draw conclusions.

# 2 Derivation of bound-state equations in the used model

We use the Wick-Cutkosky model to describe the dynamics of two scalar particles of opposite charge exchanging a neutral scalar particle. In the original model by Wick and Cutkosky [4] the exchanged particle is massless. It is possible to extend this model to a version where particles with a certain mass are exchanged. In our model we have taken bosons of equal mass m and an exchanged particle of mass  $\mu$ , which may vanish. The Lagrangian for this system is given by:

$$\mathcal{L} = \partial_{\mu} \Phi^* \partial^{\mu} \Phi - m^2 \Phi^* \Phi + \frac{1}{2} \partial_{\mu} \phi \partial^{\mu} \phi - \frac{\mu^2}{2} \phi^2 - g \phi \Phi^* \Phi , \qquad (1)$$

where g is the coupling constant,  $\Phi$  the charged field of the bosons of mass m and  $\phi$  the field of the exchanged particle.

In both forms of dynamics we have used a field theoretical method to derive the bound-state equation from this Lagrangian. In LFD there is also the possibility to make use of the so-called explicitly covariant light-front formalism (eg. Ref. [12, 6]). The bound-state equations in both methods are written in different coordinates, but it can be shown via a coordinate transformation that the equations are the same.

Through the energy-momentum tensor it is possible to find an expression for the Hamiltonian. In LFD the Hamiltonian is given by:

$$P^{-} = \int [\mathrm{d}^{3}x] \left[ \partial^{\perp}\Phi^{*}\partial^{\perp}\Phi + m^{2}\Phi^{*}\Phi + \frac{1}{2}\partial^{\perp}\phi\partial^{\perp}\phi + \frac{\mu^{2}}{2}\phi^{2} + g\phi\Phi^{*}\Phi \right] . (2)$$

Here  $\partial^{\perp} = (\partial^1, \partial^2)$  and the integration element  $[d^3x] = dx^- d^2x^{\perp}$ .

In IFD the Hamiltonian is given by:

$$H = \int d^3x \left[ \partial^0 \Phi^* \partial^0 \Phi + \vec{\nabla} \Phi^* \vec{\nabla} \Phi + m^2 \Phi^* \Phi \right]$$
  
+ 
$$\frac{1}{2} \partial^0 \phi \partial^0 \phi + \frac{1}{2} (\vec{\nabla} \phi)^2 + \frac{\mu^2}{2} \phi^2 + g \phi \Phi^* \Phi \right] .$$
 (3)

Here the integration element  $d^3x$  is defined as  $d^3x = dx^1dx^2dx^3$ , as usual.

Following the standard procedures explained in Ref. [2] for LFD and Ref. [15] for IFD, we can expand the free fields  $\phi$  and  $\Phi$  as follows

$$\phi(x) = \int \{d^3k\} \left(a(k)e^{-ikx} + a^{\dagger}(k)e^{ikx}\right), \tag{4}$$

$$\Phi(x) = \int \{d^3k\} \left(b(k)e^{-ikx} + d^{\dagger}(k)e^{ikx}\right). \tag{5}$$

Here a annihilates the exchanged neutral scalar particle, b annihilates the charged boson and d annihilates the boson with opposite charge.

The difference in the free field expansion in both forms of dynamics lies in the integration element and in the interpretation of the operators a, b and d. In LFD the integration element is

$$\{d^3k\} = \frac{[d^3k]}{(2\pi)^{3/2}\sqrt{2k^+}}.$$
 (6)

In LFD we define the integration element in momentum space  $[d^3k]$  in a similar way as we did in coordinate space:  $[d^3k] = dk^+d^2k^{\perp}$ . In IFD the integration element is given by

$$\{d^3k\} = \frac{d^3k}{(2\pi)^{3/2}\sqrt{2E(k,m)}}.$$
 (7)

Here  $d^3k$  is the usual integration element in IFD and the energy is given by  $E(k,m) = \sqrt{\vec{k}^2 + m^2}$ .

Substituting the free field expansions into Eqs. (2) or (3), we can find an expression for the Hamiltonian. Using normal ordering, we can write down the Hamiltonian, which can be split into two parts, a free part and a part containing the interaction. In Eqs. (8) and (9) the expressions are given in LFD:

$$P_{\text{free}}^{-} = \int [d^{3}k] \left( \frac{k_{\perp}^{2} + \mu^{2}}{2k^{+}} a^{\dagger}(k) a(k) + \frac{k_{\perp}^{2} + m^{2}}{2k^{+}} \left[ b^{\dagger}(k) b(k) + d^{\dagger}(k) d(k) \right] \right), \quad (8)$$

$$P_{\text{int}}^{-} = \frac{g}{(2\pi)^{3/2}} \int [d^{3}k] [d^{3}k'] \frac{\theta(k^{+} - k'^{+})}{\sqrt{8k^{+}k'^{+}(k^{+} - k'^{+})}} \times (a(k - k') \left[ b^{\dagger}(k) b(k') + d^{\dagger}(k) d(k') \right] + a^{\dagger}(k - k') \left[ b^{\dagger}(k') b(k) + d^{\dagger}(k') d(k) \right] (9)$$

The Hamiltonians in IFD are given in Eqs. (10) and (11):

$$H_{0} = \int d^{3}k \left[ E(k,m) \left( b^{\dagger}(k)b(k) + d^{\dagger}(k)d(k) \right) + E(k,\mu)a^{\dagger}(k)a(k) \right],$$

$$H_{int} = \frac{g}{(2\pi)^{3/2}} \int d^{3}k d^{3}k' \frac{1}{\sqrt{8E(k,m)E(k',m)E(k-k',\mu)}}$$

$$\times \left[ a(k-k') \left( b^{\dagger}(k)b(k') + d^{\dagger}(k)d(k') \right) + a^{\dagger}(k-k') \left( b^{\dagger}(k')b(k) + d^{\dagger}(k')d(k) \right) \right] \right]$$

In both forms of dynamics we can write down a Schrödinger like equation. In IFD we have the well-known equation  $H|\Psi\rangle = \mathcal{E}|\Psi\rangle$  where  $\mathcal{E}$  is the total energy

of the system and  $|\Psi\rangle$  is the total wave function. In LFD the Schrödinger equation is given by

$$\left(2P^{+}P^{-} - \vec{P}_{\perp}^{2}\right)|\Psi\rangle = M^{2}|\Psi\rangle. \tag{12}$$

Here  $P^- = P^-_{\rm free} + P^-_{\rm int}$  is the total Hamiltonian, M the total mass of the system and  $|\Psi\rangle$  is the total wave function.

Since it is not possible to solve a bound-state equation in full Fock space, we need to make a truncation. Here we follow the same procedure as Głazek et al. [11]. Taking only the two and three particle sectors into account, we write the total wave function as

$$|\Psi\rangle = |\varphi_2\rangle + |\varphi_3\rangle. \tag{13}$$

Using this truncation we can write the Schrödinger equation as

$$\begin{pmatrix} H_{22} & H_{23} \\ H_{32} & H_{33} \end{pmatrix} \begin{pmatrix} \varphi_2 \\ \varphi_3 \end{pmatrix} = E \begin{pmatrix} \varphi_2 \\ \varphi_3 \end{pmatrix}. \tag{14}$$

Here  $H_{22}$ ,  $H_{23}$ ,  $H_{32}$  and  $H_{33}$  connect a two particle state to a two particle state, a three particle state to a two particle state, etc.

Using this Fock-space truncation and projecting out the states gives two equations, one for the two-particle sector and one for the three-particle sector

$$\langle \varphi_2 | H_{22} | \varphi_2 \rangle + \langle \varphi_2 | H_{23} | \varphi_3 \rangle = \langle \varphi_2 | E | \varphi_2 \rangle,$$
 (15)

$$\langle \varphi_3 | H_{32} | \varphi_2 \rangle + \langle \varphi_3 | H_{33} | \varphi_3 \rangle = \langle \varphi_3 | E | \varphi_3 \rangle. \tag{16}$$

Eliminating either the two- or three-particle sector results in a bound-state equation. We have chosen to eliminate the three-particle sector and write everything in terms of the two-particle wave function, which results in

$$(E - H_{22}) |\varphi_2\rangle = H_{23} \frac{1}{E - H_{33}} H_{32} |\varphi_2\rangle.$$
 (17)

The kets  $|\varphi_2\rangle$  and  $|\varphi_3\rangle$  in Eq. (13) can be written in terms of a wave function and creation operators acting on the vacuum. We have chosen to use two different bosons in the two- and three-particle states. Then we find richer spectra, as symmetrization would remove anti-symmetric states. In the light-front formalism the wave functions are given by

$$|\varphi_2\rangle = \int [\mathrm{d}^3 p] \varphi_2(p, P - p) b^{\dagger}(p) d^{\dagger}(P - p) |0\rangle,$$
 (18)

$$|\varphi_3\rangle = \int [\mathrm{d}^3 p][\mathrm{d}^3 p']\varphi_3(p, P - p', p' - p)b^{\dagger}(p)d^{\dagger}(P - p')a^{\dagger}(p' - p)|0\rangle. (19)$$

Inserting these expressions into the bound-state equation and truncating after the second order in the coupling constant leads to an equation with four different contributions to the kernel. Two of these can be associated with the self energy

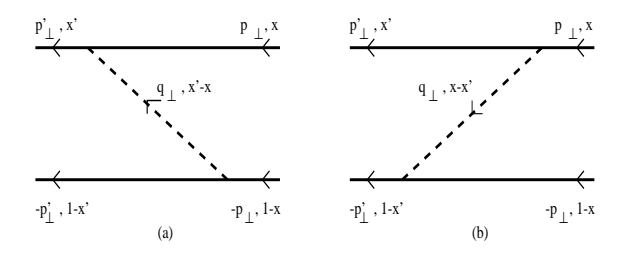


Figure 1: First order time-ordered diagrams in the ladder approximation for one particle exchange.

and are ignored in this paper. Only the terms which can be associated with the exchange of a particle between different constituents are taken into account. This means that we are working in the ladder approximation and the boundstate equation in this case becomes

$$\[ M^2 - \frac{\vec{p}_{\perp}^2 + m^2}{x(1-x)} \] \varphi_2(\vec{p}_{\perp}, x) = \frac{g^2}{(2\pi)^3} \int d^2 \vec{p}_{\perp}' dx' K(\vec{p}_{\perp}, x; \vec{p}_{\perp}', x') \varphi_2(\vec{p}_{\perp}', x') . (20)$$

Here  $K(\vec{p}_{\perp}, x; \vec{p}'_{\perp}, x')$  is the kernel of the equation, g the coupling constant and the relative variables x and  $\vec{p}_{\perp}$  are defined as:  $x = p_1^+/(p_1^+ + p_2^+)$ ,  $\vec{p}_{\perp} = (1-x)\vec{p}_{1,\perp} - x\vec{p}_{2,\perp}$ . (Note that we used an imaginary coupling to obtain an attractive interaction.)

The two terms present in the kernel of the bound-state equation can be represented graphically by two time-ordered diagrams (Fig. 1). The two time-ordered diagrams arise due to the condition that the plus-momentum of the exchanged particle should be larger than zero  $(p'^+ - p^+ > 0)$  or  $p^+ - p'^+ > 0$ . Each of these diagrams corresponds to an energy denominator which is present in the kernel of the bound-state equation. The full kernel is given by

$$K(\vec{p}_{\perp}, x; \vec{p}'_{\perp}, x') = \frac{1}{\sqrt{x(1-x)x'(1-x')}} \left( \frac{\theta(x'-x)}{2(x'-x)D_a} + \frac{\theta(x-x')}{2(x-x')D_b} \right) 21)$$

Here the theta-function gives the time-ordering and  $D_a$  and  $D_b$  are the energy denominators corresponding to left hand side and right hand side graph in Fig. 1. The expressions for these energy denominators are:

$$D_a = M^2 - \frac{\vec{p}_{\perp}^2 + m^2}{x} - \frac{\vec{p}_{\perp}'^2 + m^2}{1 - x'} - \frac{(\vec{p}_{\perp}' - \vec{p}_{\perp})^2 + \mu^2}{x' - x}, \qquad (22)$$

$$D_b = M^2 - \frac{\vec{p}_{\perp}^{\prime 2} + m^2}{x'} - \frac{\vec{p}_{\perp}^2 + m^2}{1 - x} - \frac{(\vec{p}_{\perp} - \vec{p}_{\perp}^{\prime})^2 + \mu^2}{x - x'}.$$
 (23)

In IFD the kets  $|\varphi_2\rangle$  and  $|\varphi_3\rangle$  in Eq. (13) can be written as

$$|\tilde{\varphi}_2\rangle = \int d^3p \tilde{\varphi}_2(p) b^{\dagger}(p) d^{\dagger}(-p) |0\rangle,$$
 (24)

$$|\tilde{\varphi}_3\rangle = \int d^3p d^3p' \tilde{\varphi}_3(p,p') b^{\dagger}(p) d^{\dagger}(-p') a^{\dagger}(p'-p) |0\rangle.$$
 (25)

After doing calculations similar to those described above we get, when working in the centre of mass system, the bound-state equation in the IFD formalism

$$\left[\mathcal{E} - 2\sqrt{\vec{p}^{2} + m^{2}}\right] \tilde{\varphi}_{2}(\vec{p}) = \frac{g^{2}}{(2\pi)^{3}} \int d^{3}p' \frac{1}{\mathcal{E} - \sqrt{\vec{p}'^{2} + m^{2}} - \sqrt{\vec{p}^{2} + m^{2}} - \sqrt{(\vec{p}' - \vec{p})^{2} + \mu^{2}}} \times \frac{\tilde{\varphi}_{2}(\vec{p}')}{4\sqrt{\vec{p}'^{2} + m^{2}}\sqrt{\vec{p}^{2} + m^{2}}\sqrt{(\vec{p}' - \vec{p})^{2} + \mu^{2}}}.$$
(26)

The bound states in the ladder approximation are found by solving Eq. (20) and (26) respectively.

# 3 Characterization of states

After having found the bound states, we must identify the states and assign quantum numbers to them. This can be done by using the squared orbital angular momentum operator  $\vec{L}^2$ . In the IFD approach there is no problem to identify the states. The orbital angular momentum operator  $\vec{L}$  is kinematical and both the orbital angular momentum quantum number l and the magnetic quantum number m are good quantum numbers. This in contrast to the LFD approach, where  $\vec{L}$  is dynamical. This leads to the fact that only the helicity l is a good quantum number and that l is not.

It is possible to approximate the  $\vec{L}$ -operator in LFD by first transforming the light-cone variables  $(x, \vec{p}_{\perp})$  into the variables  $(p_z, \vec{p}_{\perp})$ . Note that this object is not a true three-dimensional vector, as its components do not transform properly under all 3D rotations. The transformation we use was first introduced by Terent'ev [13] and is given by

$$x = \frac{\sqrt{m_1^2 + \vec{p}^2} + p_z}{\sqrt{m_1^2 + \vec{p}^2} + \sqrt{m_2^2 + \vec{p}^2}}.$$
 (27)

Note that this transformation is exact for free particles. Its inverse is given by

$$p_z = \left(x - \frac{1}{2}\right) \left[\frac{\vec{p}_{\perp}^2 + m_1^2}{x} + \frac{\vec{p}_{\perp}^2 + m_2^2}{1 - x}\right]^{1/2} - \frac{m_1^2 - m_2^2}{2\left[\frac{\vec{p}_{\perp}^2 + m_1^2}{x} + \frac{\vec{p}_{\perp}^2 + m_2^2}{1 - x}\right]^{1/2}} (28)$$

After making this transformation, we can approximate the orbital angular momentum operator  $\vec{L}$  by using

$$\vec{L} = i\vec{p} \times \vec{\nabla}_p \,. \tag{29}$$

To characterize a state we have found, we calculate the percentage of a specific angular momentum state (i.e. S, P, D, ...) present in this state. This is done by taking the inner product with a spherical harmonic  $Y_{lm}$ , thus projecting

the wave function on a radial function. In this way we can calculate for every angular momentum quantum number l whether it is present in a calculated state and if so, how big its contribution to that state is. If the overlap is over 85% we characterize the calculated state with the quantum number l. We realize that this way of determining the angular momentum is only approximate.

# 4 Method of solution

We solved both bound-state equations (in LFD and IFD) numerically. This was done by integrating out the angular dependence and making an expansion into basis functions.

The LFD wave function  $\varphi_2(\vec{p}_{\perp}, x)$  in the bound-state equation, Eq. (20), depends on both the momentum and the orientation of  $\vec{p}_{\perp}$  in space. It is possible to expand this wave function in eigenfunctions of  $L_z$ ,

$$\varphi_2(\vec{p}_{\perp}, x) = \sum_h \frac{1}{\sqrt{\frac{p_{\perp}^2 + m^2}{x(1-x)} - M^2}} \psi_h(p_{\perp}, x) \chi_h(\phi). \tag{30}$$

where h is the helicity and the factor  $1/\sqrt{\frac{p_1^2+m^2}{x(1-x)}-M^2}$  is introduced to symmetrize the integral equation. The angular part of a wave function with fixed helicity h is

$$\chi_h(\phi) = \frac{1}{\sqrt{2\pi}} \exp(-ih\phi). \tag{31}$$

We use it to integrate out the angular dependence in the integral equation, Eq. (20).

As we can see from Eq. (30) the momentum dependent wave functions in LFD depend on both the perpendicular and plus component of the momenta. For the x-dependence of this wave function we have used cubic spline functions Ref. [16, 17] and for the  $p_{\perp}$ -dependence we have used a basis which contains Jacobi polynomials, viz

$$\psi_{kl}(p_{\perp}) = \bar{N}_{kl} p^l \left(\frac{\mu_{sc}}{p^2 + \mu_{sc}^2}\right)^{l+3/2} P_k^{(l+1,l)} \left(\frac{p^2 - \mu_{sc}^2}{p^2 + \mu_{sc}^2}\right). \tag{32}$$

Here  $\mu_{sc}$  is a scaling parameter, l = 0, 1, 2, ..., and  $\bar{N}_{kl}$  is the normalization constant, which is given by

$$\bar{N}_{kl} = \frac{2\sqrt{\mu_{sc}k!(k+2l+1)!}}{\Gamma(k+l+1)}$$
 (33)

These functions are similar to functions which were first introduced by Olsson and Weniger (see below). We have chosen them because they have the right behaviour at the origin and for  $p \to \infty$ .

For technical reasons we symmetrized the integral equation using the transformation given in Eq. (30). The kernel of the symmetrized bound-state equation for fixed helicity h is given by:

$$K(p_{\perp}, x; p'_{\perp}, x') = \frac{p_{\perp}^{3/2} p'_{\perp}^{3/2}}{\sqrt{M^2 x (1 - x) - (p_{\perp} + m^2)} \sqrt{M^2 x' (1 - x') - (p'_{\perp}^2 + m^2)}} \times \left[ \frac{2\pi \theta(x' - x)}{2(x' - x) D'_a} \frac{1}{\sqrt{1 - \left(\frac{2p_{\perp} p'_{\perp}}{(x' - x) D'_a}\right)^2}} \left( \frac{\sqrt{1 - \left(\frac{2p_{\perp} p'_{\perp}}{(x' - x) D'_a}\right)^2 - 1}}{\frac{2p_{\perp} p'_{\perp}}{(x' - x) D'_a}} \right)^{|h|} \right] + \frac{2\pi \theta(x - x')}{2(x - x') D'_b} \frac{1}{\sqrt{1 - \left(\frac{2p_{\perp} p'_{\perp}}{(x' - x') D'_b}\right)^2}} \left( \frac{\sqrt{1 - \left(\frac{2p_{\perp} p'_{\perp}}{(x - x') D'_b}\right)^2 - 1}}{\frac{2p_{\perp} p'_{\perp}}{(x - x') D'_b}} \right)^{|h|} \right], \quad (34)$$

where  $D'_a$  and  $D'_b$  are given by

$$D_a' = M^2 - \frac{p_{\perp}^2 + m^2}{x} - \frac{p_{\perp}'^2 + m^2}{1 - x'} - \frac{p_{\perp}'^2 + p_{\perp}^2 + \mu^2}{x' - x}, \tag{35}$$

$$D_b' = M^2 - \frac{p_{\perp}'^2 + m^2}{x'} - \frac{p_{\perp}^2 + m^2}{1 - x} - \frac{p_{\perp}^2 + p_{\perp}'^2 + \mu^2}{x - x'}.$$
 (36)

Since we have integrated out the angular dependence the vector character of the momenta in these equations has disappeared. Note that in the kernel the absolute value of the helicity is present, which implies that states with opposite helicities are degenerate.

The wave functions in IFD depend on the three-momentum (see e.g. Eq. (26)). In this case we can expand the wave functions into spherical harmonics

$$\tilde{\varphi}_2(\vec{p}) = \sum_{lm} Y_{lm}(\hat{p})\phi_l(p). \tag{37}$$

Note that we can integrate out both angles  $\theta$  and  $\phi$ , whereas in LFD we could only integrate out one angle,  $\phi$ . For the momentum dependent part of the wave function we can make an expansion into basis functions as well. Here we use a basis which was first introduced by Olsson and Weniger [18]

$$\psi^{OW}(p) = N_{kl} p^l \left( \frac{\mu_{sc}}{p^2 + \mu_{sc}^2} \right)^{l+2} P_k^{(l+3/2, l+1/2)} \left( \frac{p^2 - \mu_{sc}^2}{p^2 + \mu_{sc}^2} \right).$$
(38)

Here  $\mu_{sc}$  is a scaling parameter, l = 0, 1, 2, ..., and the normalization constant  $N_{kl}$  is given by

$$N_{kl} = \frac{2\sqrt{\mu_{sc}k!(k+2l+2)!}}{\Gamma(k+l+3/2)}.$$
 (39)

We symmetrize the integral equation by using the transformation

$$\phi_l(p) = \frac{\bar{\phi}_l(p)}{\sqrt{\mathcal{E} - 2\sqrt{p^2 + m^2}}}.$$
(40)

After symmetrizing the equation and integrating out the angular dependence the kernel of the bound-state equation in IFD becomes

$$\tilde{K}(p,p') = \frac{2\pi}{\sqrt{\mathcal{E} - 2\sqrt{p^2 + m^2}}} \frac{V_l(p,p')}{\sqrt{\mathcal{E} - 2\sqrt{p'^2 + m^2}}} \frac{4\sqrt{p^2 + m^2}\sqrt{p'^2 + m^2}}{\sqrt{p'^2 + m^2}} \frac{41}{\sqrt{p'^2 + m^2}} \frac{V_l(p,p')}{\sqrt{p'^2 + m^2}} \frac{V_l(p,p')}{\sqrt{p'^2$$

Here l is the angular momentum quantum number and  $V_l(p, p')$  is obtained by integrating over the angle between  $\vec{p}$  and  $\vec{p}'$  and is given by

$$V_{l}(p, p') = \int \frac{\mathrm{d}(\hat{p} \cdot \hat{p'}) P_{l}(\hat{p} \cdot \hat{p'})}{\mathcal{E} - \sqrt{p^{2} + m^{2}} - \sqrt{p'^{2} + m^{2}} - \sqrt{p^{2} + p'^{2} + \mu^{2} - 2pp'(\hat{p} \cdot \hat{p'})}} \times \frac{1}{\sqrt{p^{2} + p'^{2} + \mu^{2} - 2pp'(\hat{p} \cdot \hat{p'})}},$$
(42)

where  $P_l(\hat{p} \cdot \hat{p'})$  is a Legendre polynomial.

#### 5 Numerical results

First we studied the accuracy of the matrix elements. Using enough integration points allows us to calculate the matrix elements with an accuracy of at least six decimal places. We studied the convergence of the spectra with respect to the number of basis functions, i.e., spline functions and Olsson Weniger like functions in LFD and the functions introduced by Olsson and Weniger in the case of IFD. In LFD we found that 14 spline functions or more and eight Olsson Weniger like functions or more give an accuracy of at least three decimal places for the lowest state for any l. The states with principal quantum number n=3 have an estimated absolute error of 0.004. In IFD taking 20 basis functions or more gives an accuracy of four decimal places in all cases considered.

Taking more basis functions into account gives some variation in the absolute values of the masses. The relative position of the bound states does not change, which means that the spectra are not changed qualitatively.

We have also compared our calculations in LFD with those of Mangin-Brinet et al. [6]. They have calculated the ground-state masses only and we have compared our calculated ground-state masses with those given in Ref. [6]. We have to remark that in that paper a coupling constant  $\alpha$  is used, where  $\alpha = g^2/(16\pi m^2)$ . In Table 1 our calculated ground-state masses are compared with the values from Ref. [6] for different values of the coupling constant. For smaller values of g we find the same bound-state masses, while for larger values we find

Table 1: Comparison of the ground-state masses given in Ref. [6] (M.B.) and those obtained in the present calculation for different values of the coupling constant.

$\alpha$	g	mass M.B.	mass this calc.
6.0	17.36	0.820	0.811
5.0	15.85	1.160	1.156
4.0	14.18	1.415	1.412
2.0	10.03	1.790	1.788
1.0	7.09	1.923	1.922
0.5	5.01	1.973	1.973

somewhat smaller masses. As in Ref. [6] the masses are given in three decimal places only, we conclude that our calculations are essentially in agreement with those of Mangin-Brinet et al.

#### 5.1 Spectra

For different values of the coupling constant we have calculated the spectra in the case of massless exchange. In the LFD formalism we have calculated the bound states for different helicities and afterwards determined the corresponding orbital angular momentum quantum number. Here we have used eight basis functions for the  $p_{\perp}$ -dependence and 14 spline functions for the plus-momentum dependence of the wave function. In the IFD formalism the bound states are calculated with l as a good quantum number and by using 25 Olsson Weniger functions.

In Fig. 2 the spectra are plotted for coupling constant g=17.36, 14.18, and 10.03, which correspond to  $\alpha=6$ , 4, and 2. We have only plotted the cases l=0,1,2. We should remark that in Fig. 2 the spectrum for  $\alpha=6$  is not completely shown. (We have left out the ground state to get a better view of the rest of the spectrum.) Due to the breaking of manifest rotational invariance in LFD the P-states and D-states are split. The center of gravity of these split levels is plotted in Fig. 2 as a dashed line and the values corresponding to this center of gravity are given in Table 2. Looking at the S-states and the dashed lines in Fig. 2 we observe a more or less similar pattern as found in IFD (Fig. 3). Looking at the spectra for different coupling constants we see that the binding becomes less when the coupling constant becomes smaller. This is the same in both IFD and LFD. Comparing between the different formalisms we see that the states in the LFD formalism have more binding.

If instead of massless exchange  $\mu \neq 0$  is considered, one may expect the masses to increase. This is borne out by comparing  $\mu = 0$  and  $\mu = 0.15$ . The comparison is done for all three values of the coupling constant used above, i.e.,  $\alpha = 6$ , 4 and 2. In Table 3 the LFD calculated masses with orbital angular momentum quantum number l = 0, 1, 2 ( $\mu = 0$  and  $\mu = 0.15$ ) are compared

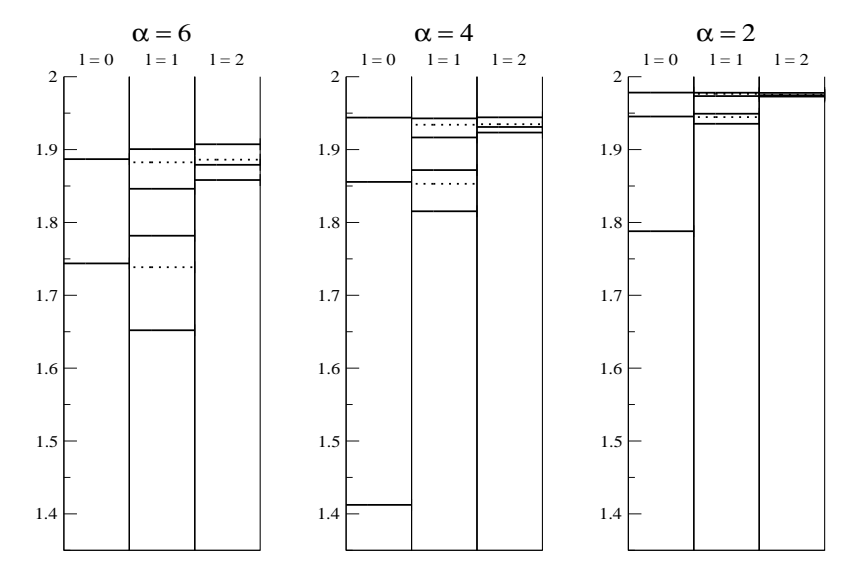


Figure 2: Spectra in LFD in the case  $\mu = 0$  for different coupling constants.

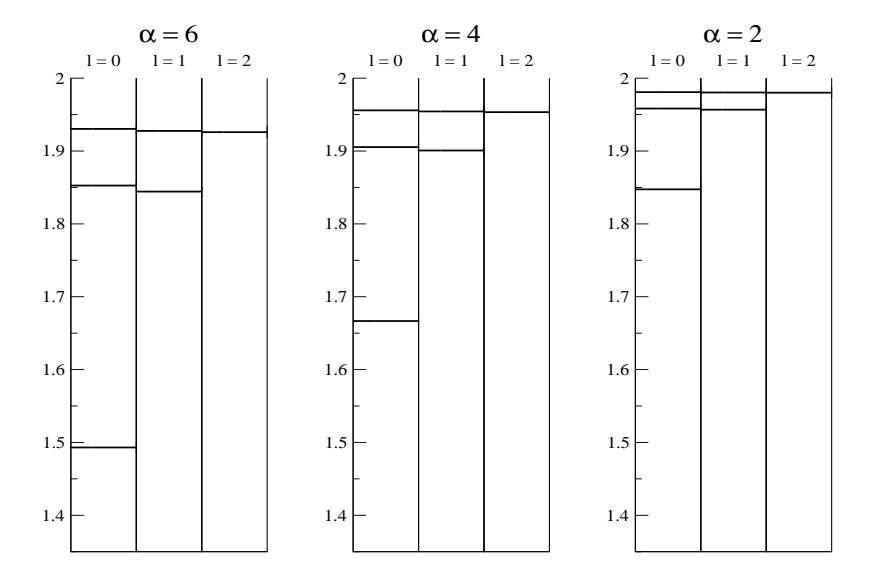


Figure 3: Spectra in IFD in the case  $\mu=0$  for different coupling constants.

Table 2: Masses corresponding to the center of gravity for the P-states and D-states in LFD for  $\mu = 0$  and coupling constants g = 17.36, 14.18, and 10.03.

g=1	g = 17.36		g = 14.18			g = 10.03		
l = 0			l = 0			l = 0		
0.811	1S		1.412	1S		1.788	1S	
1.744	2S		1.856	2S		1.945	2S	
1.885	3S		1.936	3S		1.978	3S	
l =	1		l=1			l = 1		
1.739	2P		1.853	2P		1.945	2P	
1.883	3P		1.934	3P		1.977	3P	
l=2			l =	2		l = 2		
1.886	3D		1.935	3D		1.976	3D	

to those calculated in IFD for a coupling constant g=17.36 ( $\alpha=6$ ). The calculated masses for a coupling constant g=14.18 ( $\alpha=4$ ) and g=10.03 ( $\alpha=2$ ) are given in Table 4 and 5. In all these tables the quantum numbers of the states are given as well as the masses.

Table 3: Comparison of the calculated mass spectra in LFD and IFD in the case of massless and massive exchange for a coupling constant g = 17.36 ( $\alpha = 6$ ).

	$\mu = 0.0$										
LFI	)	IFD		LFI	)	IFD	)	LFD		IFD	
	l =	=0			l = 1			l=2			
0.811	1S	1.4931	1S	1.652	2P	1.8443	2P	1.858	3D	1.9259	3D
1.744	2S	1.8526	2S	1.782	2P			1.879	3D		
1.885	3S	1.9304	3S	1.846	3P	1.9276	3P	1.907	3D		
-		-		1.901	3P			-		-	
					μ =	= 0.15					
LFI	)	IFD		LFI	LFD		IFD		)	IFD	)
	l =	=0			l = 1			l =	=2		
0.923	1S	1.5384	1S	1.753	2P	1.9153	2P	-		-	
1.846	2S	1.9276	2S	1.870	2P			-		-	

As we already saw in Fig. 2, the states have less binding for decreasing coupling constant and we find only a few bound states in the case of g = 10.03. Tables 3, 4, and 5 show the same effect. From these results it also becomes clear that the states in the case of massless exchange have more binding than those for  $\mu = 0.15$ . Especially in the case of l = 1 or 2 the binding is sometimes so small that we did not succeed in calculating the bound-state mass with the

Table 4: Comparison of the calculated bound-state masses in LFD and IFD in the case of massless and massive exchange for a coupling constant g = 14.18 ( $\alpha = 4$ ).

	$\mu = 0.0$										
LFI	)	IFD		LFD IFD			LFD		IFD		
	l :	=0			l =	= 1			l =	=2	
1.412	1S	1.6666	1S	1.815	2P	1.9007	2P	1.923	3D	1.9534	3D
1.856	2S	1.9054	2S	1.872	2P			1.931	3D		
1.944	3S	1.9558	3S	1.917	3P	1.9543	3P	1.944	3D		
-		-		1.943	3P			-		-	
					$\mu =$	= 0.15					
LFI	)	IFD	1	LFI	LFD IFD		)	LFD		IFD	)
	l :	=0			= 1			l =	=2		
1.477	1S	1.7093	1S	1.898	2P	1.9628	2P	-		-	
1.937	2S	1.9690	2S	1.945	2P			-		-	

number of basis functions we have used.

#### 5.2 Wave functions

Besides the spectra we calculated the wave functions corresponding to the bound states. In Fig. 4 the 2-D LFD wave functions of the 1S, 2S and 2P states for g=17.36 and  $\mu=0$  are given. These figures show the variation of the wave function with x (or  $p^+$ ) and  $|\vec{p}_{\perp}|$ . We see that the wave function goes asymptotically to zero when  $|\vec{p}_{\perp}|$  becomes large.

In Fig. 5 the wave functions corresponding to the 1S, 2S, and 3S states are plotted for all three values of the coupling constant in the case of massless exchange. This figure shows that the wave function becomes flatter and broader when the coupling constant increases. All functions go asymptotically to zero and show the correct number of nodes; i.e. zero nodes for the 1S state, one node for the 2S-state etc.

In the case of the S-states, the helicity can only be equal to zero. This in contrast to the P- and D-states where we have helicity -1, 0 and 1 (P-states) and -2, -1, 0, 1 and 2 (D-states). In our calculations we have worked with positive helicities only. We can do this because of the fact that only the absolute value of the helicity is present in the kernel, Eq. (34). In Fig. 6 the 2P, 3P, and 3D states for all (positive) helicities are plotted in the case of  $\mu=0$  for coupling constant  $\alpha=6,4,2$ . As could be expected, the radial wave functions depend on the helicity, which is again due to the breaking of rotational invariance. The comparison between the radial wave functions calculated in LFD and IFD is made in Fig. 5.2. In this figure the wave functions are plotted for a coupling

Table 5: Comparison of the calculated bound-state masses in LFD and IFD in the case of massless and massive exchange for a coupling constant g = 10.03 ( $\alpha = 2$ ).

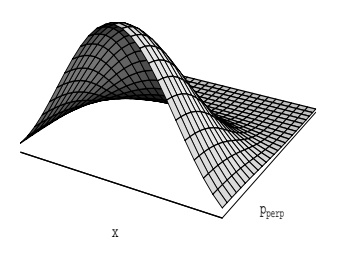
	$\mu = 0.0$											
LFI	)	IFD		LFD IFD			LFD		IFD			
	l =	=0			l =	= 1			l=2			
1.788	1S	1.8474	1S	1.935	2P	1.9568	2P	1.973	3D	1.9801	3D	
1.945	2S	1.9583	2S	1.949	2P			1.975	3D			
1.978	3S	1.9808	3S	1.973	3P	1.9803	3P	1.978	3D			
-		-		1.978	3P			-		-		
					μ =	= 0.15						
LFI	)	IFD		LFI	LFD			LFI	)	IFD	)	
l = 0			l =	= 1			l =	= 2				
1.833	1S	1.8849	1S	1.992	2P	1.9995	2P	-		-		
1.995	2S	1.9982	2S	1.998	2P	-		-		-		

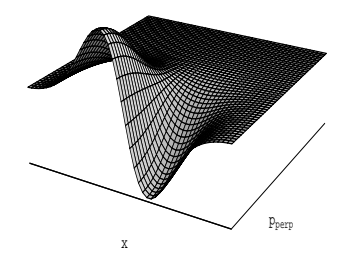
constant g = 17.36 only. Comparing the plots in Fig. 5.2 we see that the wave function calculated in the LFD formalism is flatter and broader than the wave function calculated in IFD.

# 6 Discussion and conclusions

We calculated the bound-state spectrum of the Wick-Cutkosky model in the ladder approximation both in light-front dynamics and in instant-form dynamics. We used as a variational method an expansion of the wave function in spline functions for the x dependence and an orthonormal set for the  $p_{\perp}$  coordinate in LFD. Likewise, we used a similar set for the radial wave functions in IFD. We checked the absolute convergence of the spectra and also convinced ourselves that the relative positions of the mass eigenvalues will very probably not change at all when the number of basis functions would be increased above what we have used.

As rotational invariance is broken in LFD by cutting off the Fock-space expansion, we cannot expect the correct multiplet structure to appear in the ladder approximation. Moreover, because the angular-momentum operator is dynamical, we cannot immediately determine the angular momentum quantum number l of the states found in LFD. Using Terent'ev's transformation, which is approximate in the bound-state (off-energy-shell) case, we were able to characterize the bound states by calculating their overlaps with the spherical harmonics  $Y_{lm}(\hat{p})$ . Following this procedure, we could estimate the degree of breaking of rotational invariance in LFD. Not surprisingly, rotational symmetry is less violated for small values of the coupling constant than for strong coupling.





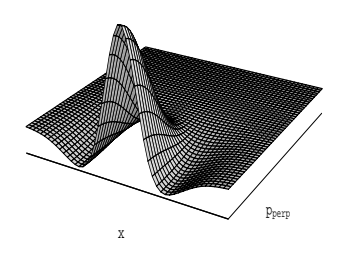


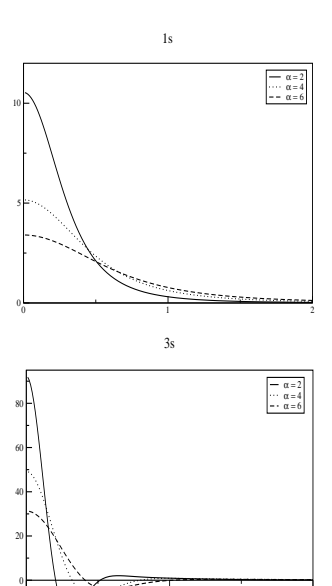
Figure 4: LFD wave functions (1S, 2P, 2S) corresponding to the first three states in the case m = 1.0,  $\mu = 0.0$  and g = 17.36

The well-known O(4) symmetry of the WC-model is violated in the ladder approximation in both LFD and IFD. If one computes the centers of gravity of the states with the same l and helicities h = -l, ..., l, one finds that the breaking of O(4) symmetry in LFD and IFD are quite similar.

In all cases we considered, the masses calculated in LFD are smaller than in IFD. One might try to explain this fact by pointing out that the Fock-space expansion converges more rapidly in LFD than in IFD, as shown in Ref. [3], but one must keep in mind that in the latter paper the Yukawa model was investigated, so one cannot be absolutely certain of the validity of this argument for the WC-model. Calculations done by Cooke and Miller [9] and Schoonderwoerd et al. [3] show that the breaking of rotational invariance in the Yukawa model is partially restored by including the box diagram.

Although in the cases where the coupling constant is large, the bound systems are certainly relativistic with binding energies of the same order as the masses of the constituents, we find even then that the binding energies follow the nonrelativistic rule  $E_n = E_1/n^2$  remarkably well. This feature is illustrated in Table 6. For very weak coupling,  $\alpha = 0.5$  and 1.0, we see a similar pattern for the Salpeter equation, see Table 7, although in this case the binding is much larger than in the LFD case.

The potential used is not bounded from below and shows a collapse of the wave function above a critical value of the coupling constant, see Ref. [19]. In the literature a critical value of  $\alpha \approx 1.27$  can be found [20]. Looking at Table 7 we



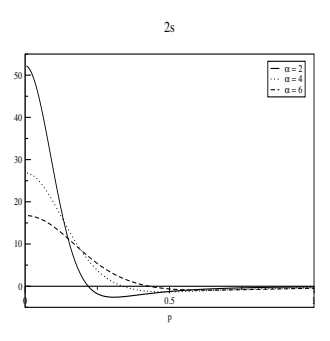


Figure 5: LFD radial wave functions corresponding to the 1S, 2S and 3S states for  $\alpha = 6$ , 4 and 2.

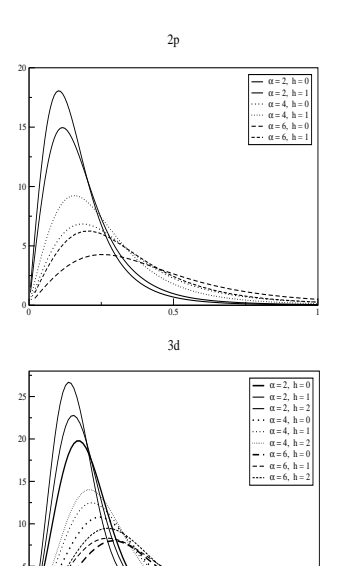
see that the ground-state mass for  $\alpha=2$  has dropped enormously, illustrating the collapse.

An analytical solution of the Wick equation in the weak-binding limit is given by Feldman et al. [21]. In Table 8 the bound-state masses are given for two values of the coupling constant,  $\alpha=0.5$  and  $\alpha=1$ , calculated with the expression for the binding energy given in Ref. [21]. For these two values of the coupling constant we also calculated the bound-state masses in LFD and IFD (see Table 8) for l=0 only.

In his paper Cutkosky [4] gives a plot of his numerical results obtained in the WC-model. From his figure we read off masses for different values of the coupling constant (row 'WC' in Table 9). In a similar way we read off the masses from Fig. 2 in Ref. [8]. Looking at this figure we see that only the results by Ji are not underestimating the WC-model masses. In Table 9 we give the masses which we read off from the curve labelled 'Ji'. For comparison we also give the masses of the 1S state calculated in the LFD approach and those calculated with the analytical expression given by Ref. [21] (row 'FFT' in Table 9). Here we should remark that the analytical expression is only valid for small values of the coupling constant.

From Table 9 we see that the masses calculated by Ji overestimate the bound-state masses for the WC-model. We also see that the analytical expression of [21] is only valid for small values of the coupling constant  $\alpha$ .

Besides the mass spectrum we have also calculated both the two-dimensional



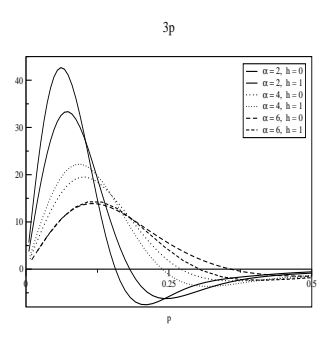


Figure 6: LFD radial wave functions corresponding to the 2P, 3P and 3D states for  $\alpha=6,\,4$  and 2.

and radial wavefunctions. Breaking of rotational invariance is clearly seen in the LFD case.

# References

- [1] P.A.M. Dirac, Rev. Mod. Phys. **21**, 392 (1949)
- [2] S.J. Brodsky, H.C. Pauli, and S.S. Pinsky, Phys. Rept. **301**, 299 (1998)
- [3] N.C.J. Schoonderwoerd, B.L.G. Bakker, and V.A. Karmanov, Phys. Rev. C58, 3093 (1998)
- [4] G.C. Wick, Phys. Rev., 96, 1124 (1954); R.E. Cutkosky, Phys. Rev., 96, 1135 (1954)
- [5] N. Nakanishi, Prog. Theor. Phys. Suppl. 95, 1 (1988)
- [6] M. Mangin-Brinet and J. Carbonell, Phys. Lett. **B474**, 237 (2000);M. Mangin-Brinet, PhD-thesis (2001)
- [7] C.R. Ji and R.J. Furnstahl, Phys. Lett. **B167**, 11 (1986)
- [8] B. Ding and J. Darewych, J. Phys. **G26**, 907 (2000)

Table 6: Comparison of the calculated binding energies (LFD and IFD) with  $E_1/n^2$  for the S-states at  $\mu = 0$  in the case of  $\alpha = 6$ , 4 and 2.

	LFD								
	$\alpha$ =	-	$\alpha$ =		$\alpha = 2$				
	calc	$E_1/n^2$	calc	$E_1/n^2$	calc	$E_1/n^2$			
$E_1$	1.189	1.189	0.588	0.588	0.212	0.212			
$E_2$	0.256	0.297	0.144	0.147	0.055	0.053			
$E_3$	0.115	0.132	0.056	0.065	0.022	0.024			
			IFD						
	α =	= 6	$\alpha$ =	= 4	$\alpha$ =	= 2			
	calc	$E_1/n^2$	calc	$E_1/n^2$	calc	$E_1/n^2$			
$E_1$	0.5069	0.5069	0.3334	0.3334	0.1526	0.1526			
$E_2$	0.1474	0.1274	0.0946	0.0834	0.0417	0.0382			
$E_3$	0.0696	0.0566	0.0442	0.0370	0.0192	0.0170			

Table 7: Bound state-masses calculated with a relativistic Salpeter equation.

	$\alpha = 0.5$	$\alpha = 1$	$\alpha = 2$	$\alpha = 0.5$	$\alpha = 1$	$\alpha = 2$	$\alpha = 0.5$	$\alpha = 1$	$\alpha = 2$
n	l = 0				l = 1		l=2		
1	1.9332	1.6825	0.4373	1.9842	1.9352	1.7092	1.9930	1.9719	1.8829
2	1.9836	1.9251	1.6079	1.9930	1.9712	1.8710	1.9961	1.9842	1.9339
3	1.9928	1.9683	1.8419	1.9961	1.9839	1.9289	1.9975	1.9899	1.9578
4	1.9960	1.9827	1.9171	1.9975	1.9897	1.9553	1.9983	1.9930	1.9709
5	1.9975	1.9891	1.9495	1.9984	1.9929	1.9694	1.9992	1.9948	1.9787

- [9] J.R. Cooke, G.A. Miller, and D.R. Phillips, Phys. Rev. C61, 064005 (2000);
   J.R. Cooke and G.A. Miller, Phys. Rev. C62, 054008 (2000)
- [10] T. Nieuwenhuis and J.A. Tjon, Phys. Rev. Lett. 77, 814 (1996)
- [11] S. Głazek, A. Harindranath, S. Pinsky, J. Shigemitsu, and K. Wilson, Phys. Rev. D47, 1599 (1993)
- [12] M.G. Fuda, Annals of Physics, 197, 265 (1990); and Annals of Physics,
  231, 1 (1994); M.G. Fuda and Y. Zhang, Phys. Rev. C51, 23 (1995); M.G. Fuda, Phys. Rev. C52, 1260 (1995)
- [13] M.V. Terent'ev, Sov. J. Nucl. Phys., 24, 106 (1976); B.L.G. Bakker,
   L.A. Kondratyuk, and M.V. Terent'ev, Nucl. Phys. B158, 497 (1979)

Table 8: Bound state-masses for the Wick equation in the weak-binding limit [21] and the nS masses calculated in LFD and IFD.

		$\alpha = 0.5$	Ó		$\alpha = 1$	
n	Wick	LFD	IFD	Wick	LFD	IFD
1	1.965	1.973	1.9760	1.750	1.922	1.9364
2	1.991	1.999	1.9939	1.938		1.9831
3	1.996		1.9996	1.972		1.9931

Table 9: Comparison of different calculations of the 1S state for various values of the coupling constant  $\alpha$ .

	$\alpha = 0.5$	$\alpha = 1$	$\alpha = 2$	$\alpha = 4$	$\alpha = 6$
WC	1.97	1.92	1.77	1.39	0.60
LFD	1.973	1.922	1.788	1.412	0.811
Ji	1.98	1.93	1.82	1.49	1.09
FFT	1.965	1.750	-0.765	-30.241	-130.192

- [14] B.L.G. Bakker, Forms of Relativistic Dynamics, in H. Latal and W. Schweiger (Eds.), Methods of Quantization, Lecture Notes in Physics, 572, 1, Springer-Verlag, Berlin, Heidelberg 2001
- [15] C. Itzykson and J.B. Zuber, Quantum Field Theory, McGraw-Hill Inc., New York (1980)
- [16] M.G. Cox, J. Inst. Math. Applic 10, 134 (1972); ibid 15, 95 (1975)
- [17] C. de Boor, J. Approx. Theory **6**, 50 (1972)
- [18] M.G. Olsson, S. Veseli, and K. Williams, Phys. Rev. **D52**, 5141 (1995);
   E.J. Weniger, J. Math. Phys. **26**, 276 (1985)
- [19] M. van Iersel, C.F.M. van der Burgh, and B.L.G. Bakker, hep-ph/0010243
- [20] J.C. Raynal et al., Phys. Lett. **B320**, 105 (1994)
- [21] G. Feldman, T. Fulton, and J. Townsend, Phys. Rev. D7, 1814 (1973)

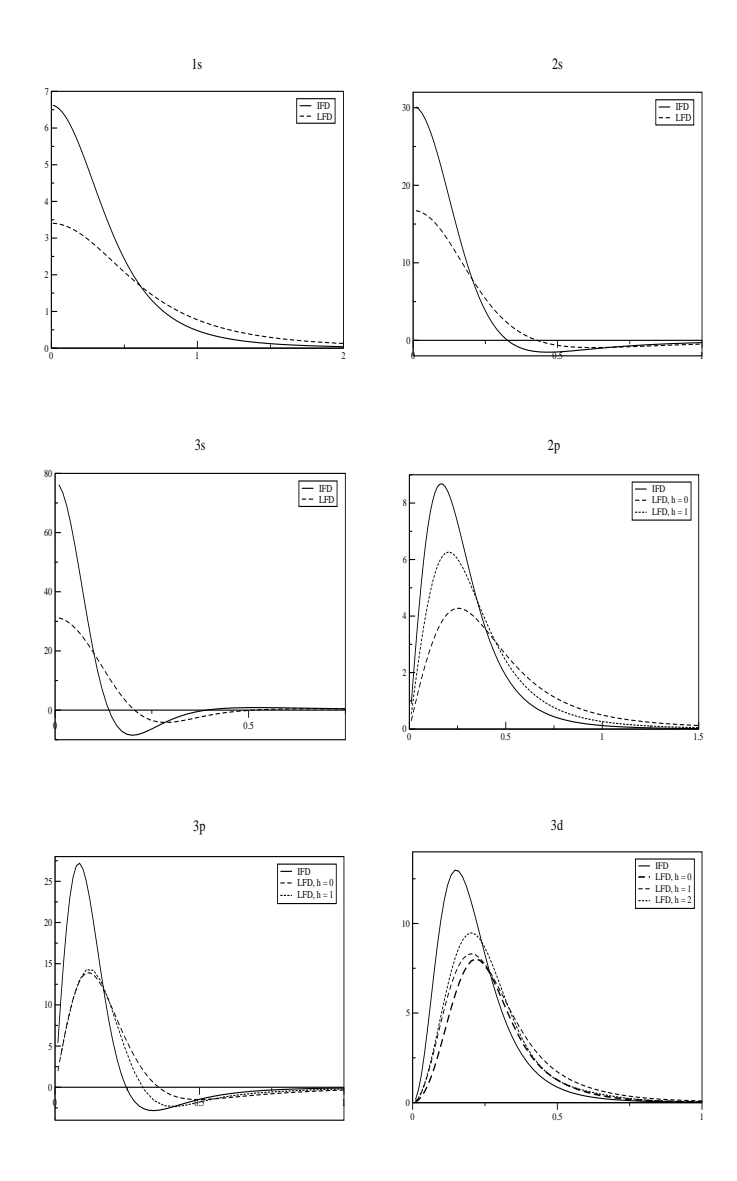


Figure 7: Comparison of the radial wave functions calculated in LFD and IFD at a coupling constant g=17.36.